AIMS Mathematics, 10(9): 21126–21158.
DOI: 10.3934/math.2025944
Received: 12 June 2025
Revised: 21 July 2025
Accepted: 24 July 2025
Published: 15 September 2025

https://www.aimspress.com/journal/Math

Research article

Hybrid multi-step fractional numerical schemes for human-wildlife zoonotic disease dynamics

Muflih Alhazmi[1,*], Safa M. Mirgani[2], Abdullah Alahmari[3] and Sayed Saber[4,5]

[1] Mathematics Department, Faculty of Science, Northern Border University, Arar, Saudi Arabia

[2] Imam Mohammad Ibn Saud Islamic University (IMSIU), College of Science Department of Mathematics and Statistics, Riyadh, Saudi Arabia

[3] Department of Mathematics, Faculty of Sciences, Umm Al-Qura University, Saudi Arabia

[4] Department of Mathematics, Faculty of Science, Al-Baha University, Al-Baha, Saudi Arabia

[5] Department of Mathematics and Computer Science, Faculty of Science, Beni-Suef University, Egypt

* **Correspondence:** Email: Muflih.alhazmi@nbu.edu.sa.

Abstract: In this study, the transmission dynamics of zoonotic diseases between baboons and humans were explored by examining increased interactions between humans and wild animals. We established the model's well-posedness through proofs of existence, uniqueness, non-negativity, and boundedness of solutions. Stability and sensitivity analyses identified key parameters affecting disease dynamics, particularly the baboon-to-human transmission rate (β_h), the human recovery rate (γ_h), and the human-side contact control parameter (H_i). The basic reproduction number (R_0) governed disease outcomes: If $R_0 < 1$, the disease died out and the infection-free equilibrium was globally asymptotically stable; if $R_0 > 1$, a unique endemic equilibrium emerged and was locally asymptotically stable, indicating the potential for disease persistence. Numerical simulations were conducted using the Multi-Step Generalized Differential Transform Method and the Adams-Bashforth-Moulton scheme, confirming the model's biological relevance. Our results indicated that sterilization reduced infected baboons by up to 40%, while food access restrictions lowered human infections by approximately 25%. By leveraging fractional calculus and advanced numerical methods, this study provides a robust framework for modeling zoonotic diseases and offers actionable insights for public health and wildlife management.

Keywords: fractional derivatives; nonlinear equations; simulation; numerical results; iterative method; zoonotic disease
Mathematics Subject Classification: 34A08, 34L99, 92D30

1. Introduction

Zoonotic diseases remain a significant challenge to global public health, particularly as human expansion encroaches upon natural habitats [1, 2]. In regions like Al-Baha, Saudi Arabia, wild baboons (genus Papio) frequently interact with humans, resulting in shared access to food and water resources, and increased potential for pathogen transmission [3–5]. These interactions expose both populations to diseases such as tuberculosis and viral infections, often transmitted through direct contact or contaminated environments [6–8].

Al-Baha's mountainous terrain and rich biodiversity make it an ecologically significant region for studying zoonotic transmission. Human-wildlife contact is common due to the proximity of settlements to forested areas such as Juniperus procera woodlands [9], which serve as habitats for disease vectors.

Mathematical models play a crucial role in understanding the dynamics of disease transmission within and between wildlife and human populations, offering valuable insights into how factors such as population size, transmission rates, and intervention strategies influence the spread of infectious diseases [10]. In addition to enabling the simulation of complex interactions, these models provide insight into how factors such as population size, disease transmission rates, and intervention strategies can influence disease spread [11]. In particular, compartmental models have been extended to fractional-order systems to incorporate memory effects, hereditary properties, and long-term environmental persistence of pathogens [12]. The Caputo derivative is especially suited for biological applications, enabling more realistic modeling of disease dynamics with non-integer memory-dependent processes [13]. Models of this kind are also widely used to study disease ecology and epidemiological patterns in wildlife populations [14], including bovine tuberculosis [8] and cutaneous leishmaniasis [15].

Examples of modeling approaches also include applications in viscoelasticity [16], quantum dynamics [17], Langevin systems [18], physics [19], and biological systems such as diabetes [20–29]. Additionally, many researchers explore modeling of computer viruses [30], zoonotic [31–35], tobacco use [36], pneumonia [37, 38], influenza [39], and infectious diseases [40], including Coronavirus [41] and emerging zoonoses [42]. Moreover, researchers have applied fractional calculus in various disease contexts, including influenza, COVID-19, and tuberculosis [43, 44]. However, not all such applications are directly relevant to zoonotic epidemiology, and we focus here on their implications for disease modeling.

For numerical solutions of fractional differential systems, schemes such as the Generalized Differential Transform Method (GDTM) [45, 46] and the Adams-Bashforth-Moulton (ABM) method [47] have demonstrated accuracy and efficiency. These approaches are particularly effective in simulating memory-influenced epidemic dynamics over extended time domains. Sadek et al. (2024) introduced novel Θ-fractional operators, expanding the framework of fractional calculus and demonstrating their efficiency in optimization problems using the Galerkin-Bell method [48]. In [49], Sadek (2023) proposed a cotangent fractional derivative, providing an alternative approach to solving complex differential equations with applications in fractional modeling. Further extending this concept, Sadek and Lazar (2023) explored the Hilfer cotangent fractional derivative and its applicability to a particular class of fractional problems, bridging the gap between classical and fractional derivatives [50]. In the context of epidemiology, Sadek et al. (2023) developed a fractional-order model to predict COVID-19 dynamics in Morocco, incorporating isolation and

vaccination strategies, where the inclusion of memory effects improved predictive accuracy [51]. Additionally, Sadek et al. (2022) applied fractional calculus to model the synthesis of TiO_2 nanopowder via the sol-gel method at low temperatures, capturing the complexities of nanopowder formation and improving process modeling in nanotechnology [52]. These contributions collectively enhance the theoretical and applied aspects of fractional calculus, demonstrating its versatility across diverse scientific domains.

To study zoonotic disease transmission between humans and baboons in the Al-Baha region, we propose a fractional-order model. Biologically realistic control strategies are incorporated into the model, such as sterilization (H_s), food access restrictions (H_f), and human-wildlife interaction (H_i) to mitigate zoonotic transmission from baboons to humans. By demonstrating the existence, uniqueness, non-negativity, and boundedness of solutions, we rigorously establish the model's well-posedness. The basic reproduction number R_0 is derived to determine threshold conditions for disease outbreak or eradication, and sensitivity analysis identifies critical parameters such as the wildlife-to-human transmission rate (β_h), the human recovery rate (γ_h), and the effectiveness of contact control (H_i). Numerical simulations using the MS-GDTM and ABM schemes validate theoretical results and assess the effectiveness of combined control strategies in lowering $\mathscr{R}_0$. While focused on the Al-Baha region, the modeling framework and findings are applicable to other areas where human-wildlife interactions pose epidemiological risks.

We aim to develop and analyze a biologically grounded, memory-aware fractional-order mathematical model that captures the transmission dynamics of zoonotic diseases between baboons and humans in ecologically sensitive regions such as Al-Baha, Saudi Arabia. By incorporating Caputo fractional derivatives, the model reflects the long-term memory effects inherent in disease progression and ecological interactions. We seek to provide a rigorous theoretical foundation for the model by establishing the existence, uniqueness, non-negativity, and boundedness of its solutions, ensuring the system is mathematically well-posed and biologically feasible. The model also accounts for realistic control interventions, including sterilization, food access restrictions, and contact reduction, to evaluate their impact on zoonotic transmission and population-level disease persistence.

Our objectives of the study include conducting equilibrium and stability analyses to determine threshold conditions for disease eradication based on the basic reproduction number $\mathcal{R}_0$, and performing sensitivity analysis to identify key parameters o-0influencing disease dynamics. To validate the analytical results and explore the temporal behavior of the system, two numerical schemes, the Multi-step Generalized Differential Transform Method (MSGDTM) and the Adams-Bashforth-Moulton (ABM) method, are implemented. The simulation results demonstrate how varying the fractional order alters the disease trajectory and amplifies the effects of interventions. This research provides actionable insights for public health authorities and environmental managers by identifying effective strategies to control zoonotic outbreaks in regions with high human-wildlife interaction.

The remainder of this paper is structured as follows: In Section 2, we provide definitions and preliminary findings and a model formulation. In Section 3, we establish the system's analytical properties. In Sections 4 and 5, we discuss stability and sensitivity analysis. In Section 6, we detail the numerical results. In Sections 7 and 8, we summarize the findings and propose directions for future research.

2. Model description

We present a compartmental zoonotic disease model that captures the transmission dynamics between human and baboon populations using fractional-order derivatives. The population of each species is subdivided into three epidemiological compartments: Susceptible, infected, and recovered. Subscripts b and h denote baboon and human compartments, respectively. To incorporate the memory and hereditary effects inherent in biological processes, the model adopts fractional-order dynamics based on the Caputo derivative.

Susceptible baboons X_b are assumed to grow logistically, constrained by the environmental carrying capacity K_b. They may become infected Y_b through intra-species interactions at a transmission rate k_b. Infected baboons recover at rate γ_b, transitioning to the recovered class Z_b. Human infections arise exclusively from zoonotic transmission: susceptible humans X_h acquire the disease through contact with infected baboons Y_b, governed by a cross-species transmission rate k_h and modulated by a contact control parameter H_i. Infected humans Y_h recover at rate γ_h, entering the recovered compartment Z_h.

The fractional-order system, governed by the Caputo derivative of order $\alpha \in (0, 1]$, is given as follows:

$$\begin{aligned}
{}^{\mathrm{C}}\mathscr{D}^{\alpha}_{0,t} X_b &= X_b\left(1 - \frac{X_b + Y_b + Z_b}{K_b}\right) - k_b X_b Y_b - H_s X_b - H_f X_b,\\
{}^{\mathrm{C}}\mathscr{D}^{\alpha}_{0,t} Y_b &= k_b X_b Y_b - \gamma_b Y_b - H_s Y_b - H_f Y_b,\\
{}^{\mathrm{C}}\mathscr{D}^{\alpha}_{0,t} Z_b &= \gamma_b Y_b - H_f Z_b,\\
{}^{\mathrm{C}}\mathscr{D}^{\alpha}_{0,t} X_h &= X_h\left(1 - \frac{X_h + Y_h + Z_h}{K_h}\right) - (1 - H_i) k_h X_h Y_b,\\
{}^{\mathrm{C}}\mathscr{D}^{\alpha}_{0,t} Y_h &= (1 - H_i) k_h X_h Y_b - \gamma_h Y_h,\\
{}^{\mathrm{C}}\mathscr{D}^{\alpha}_{0,t} Z_h &= \gamma_h Y_h,
\end{aligned} \tag{2.1}$$

with initial conditions:

$$X_b(0) = X_{b0}, \quad Y_b(0) = Y_{b0}, \quad Z_b(0) = Z_{b0}, \quad X_h(0) = X_{h0}, \quad Y_h(0) = Y_{h0}, \quad Z_h(0) = Z_{h0}.$$

Model variables and parameters:

- $X_b(t), Y_b(t), Z_b(t)$: Susceptible, infected, and recovered baboon populations.
- $X_h(t), Y_h(t), Z_h(t)$: Susceptible, infected, and recovered human populations.
- K_b, K_h: Carrying capacities of baboon and human populations, respectively.
- k_b: Transmission rate among baboons.
- k_h: Cross-species transmission rate from infected baboons to susceptible humans.
- γ_b, γ_h: Recovery rates for baboons and humans.
- H_s: Sterilization control rate reducing baboon reproduction and transmission.
- H_f: Rate of food-access restriction, reducing all baboon interactions.
- H_i: Contact-control rate between humans and baboons.

Model assumptions:

- The system is closed, with no immigration or emigration.
- Homogeneous mixing is assumed within and across the two populations.

- Humans acquire infection exclusively from infected baboons.
- Mortality due to disease is neglected; only ecological and control-driven removal occurs.
- Control measures H_s, H_f, and H_i are constant over time.
- All compartments are nonnegative and bounded by their respective carrying capacities.

Unlike classical models with integer-order derivatives, which assume instantaneous responses, fractional-order models capture:

- Long-term memory and hereditary effects, modeled via the Caputo derivative.
- Delayed feedback responses intrinsic to ecological and epidemiological processes.

The model parameters, their descriptions, and data sources are summarized in Table 1. Parameter values are informed by clinical, ecological, and behavioral data, particularly from the Al-Baha region. Clinical observations help estimate γ_h and k_h, while ecological control strategies (e.g., sterilization and restricted food provisioning) determine H_s, H_f, and H_i.

Table 1. Descriptions and sources of model parameters.

Symbol	Description	Source	Interpretation
K_b, K_h	Carrying capacities	Environmental data	Resource-based population limits
k_b	Baboons' transmission rate	Behavioral studies	Within-species contact rate
k_h	Cross-species transmission	Epidemiological data	Zoonotic contact likelihood
γ_b, γ_h	Recovery rates	Clinical records	Immunological recovery
H_s	Sterilization rate	Control policy	Birth/infection reduction in baboons
H_f	Food restriction rate	Public policy	Deterrence of human-baboon interaction
H_i	Contact reduction	Preventive strategy	Human-side protection enforcement

Fractional calculus preliminaries: The fractional integral of order $\alpha > 0$ for a function $f(t)$ is defined as:

$$I^{\alpha} f(t) = \frac{1}{\Gamma(\alpha)} \int_0^t (t-s)^{\alpha-1} f(s)\, ds,$$

where $\Gamma(\cdot)$ is the Euler Gamma function:

$$\Gamma(z) = \int_0^{\infty} e^{-t} t^{z-1}\, dt.$$

The Caputo fractional derivative of order $\alpha > 0$, for $n-1 < \alpha < n$, is given by:

$${}^{\mathrm{C}}\mathscr{D}^{\alpha}_{0,t} f(t) = \begin{cases} \dfrac{1}{\Gamma(n-\alpha)} \displaystyle\int_0^t (t-s)^{n-\alpha-1} f^{(n)}(s)\, ds, & \text{if } n-1 < \alpha < n, \\ \dfrac{d^n}{dt^n} f(t), & \text{if } \alpha = n. \end{cases}$$

This fractional-order model serves as a biologically realistic and policy-relevant framework for studying zoonotic transmission and evaluating mitigation strategies in ecologically sensitive regions such as Al-Baha.

3. Well-posedness analysis of the fractional-order model

3.1. Existence and uniqueness of solutions

We consider the fractional-order system (2.1) governed by the Caputo derivative of order $0 < \alpha \leq 1$. Let the biologically feasible region of the system be defined as:

$$\Omega = \left\{(X_b, Y_b, Z_b, X_h, Y_h, Z_h) \in \mathbb{R}^6_+ : \max\{X_b, Y_b, Z_b, X_h, Y_h, Z_h\} \leq M\right\},$$

where $M > 0$ is a positive constant depending on the system's initial conditions and parameters.

Theorem 3.1. *Let the initial condition be*

$$X_0 = (X_b(0), Y_b(0), Z_b(0), X_h(0), Y_h(0), Z_h(0)) \in \Omega.$$

Then, the fractional-order system (2.1) *admits a unique solution* $X(t) \in \Omega$ *for all* $t \geq 0$.

Proof. We rewrite system (2.1) in the standard compact Caputo form:

$${}^{\mathrm{C}}\mathscr{D}^{\alpha}_{0,t} X(t) = H(X(t)), \quad X(0) = X_0,$$

where $X(t) = (X_b, Y_b, Z_b, X_h, Y_h, Z_h)^\top \in \mathbb{R}^6_+$ is the state vector, and $H = (H_1, H_2, H_3, H_4, H_5, H_6)^\top$ is the vector-valued function defined by:

$$\begin{aligned}
H_1 &= X_b\left(1 - \frac{X_b + Y_b + Z_b}{K_b}\right) - k_b X_b Y_b - H_s X_b - H_f X_b,\\
H_2 &= k_b X_b Y_b - (\gamma_b + H_s + H_f) Y_b,\\
H_3 &= \gamma_b Y_b - H_f Z_b,\\
H_4 &= X_h\left(1 - \frac{X_h + Y_h + Z_h}{K_h}\right) - (1 - H_i) k_h X_h Y_b - H_f X_h,\\
H_5 &= (1 - H_i) k_h X_h Y_b - \gamma_h Y_h,\\
H_6 &= \gamma_h Y_h.
\end{aligned}$$

Each component $H_i \in (0, 1)$ involves polynomial or bilinear terms in the state variables, and is thus continuously differentiable in Ω. Consequently, the vector field $H(X)$ is continuous and locally Lipschitz in Ω. Therefore, by the Existence and Uniqueness Theorem for Caputo fractional differential equations (see e.g., Theorem 6.1 in Kilbas et al. [53]), the initial value problem

$${}^{\mathrm{C}}\mathscr{D}^{\alpha}_{0,t} X(t) = H(X(t)), \quad X(0) = X_0 \in \Omega,$$

has a unique solution $X(t) \in \Omega$ that exists for all $t \geq 0$. Moreover, due to the boundedness of the nonlinearities and biological positivity of the initial conditions, the solution remains within the invariant region Ω, ensuring global existence and biological feasibility. □

Theorem 3.2. *(Positivity of solutions) Let the initial conditions satisfy:*

$$X_b(0),\ Y_b(0),\ Z_b(0),\ X_h(0),\ Y_h(0),\ Z_h(0) \geq 0,$$

and suppose that the control parameter $H_i \in [0, 1]$. *Then, the solution*

$$X(t) = (X_b(t), Y_b(t), Z_b(t), X_h(t), Y_h(t), Z_h(t)) \in \mathbb{R}^6_+$$

of the fractional-order system (2.1) *remains non-negative for all* $t \geq 0$.

Proof. We examine the behavior of system (2.1) at the boundary of the non-negative orthant $\mathbb{R}^6_+$, to ensure that the solution trajectory cannot leave this domain if initialized inside it.

Let us evaluate each Caputo derivative at the point where the corresponding state variable is zero:

$$\begin{aligned}
{}^{\mathrm{C}}\mathscr{D}^{\alpha}_{0,t} X_b\Big|_{X_b=0} &= 0,\\
{}^{\mathrm{C}}\mathscr{D}^{\alpha}_{0,t} Y_b\Big|_{Y_b=0} &= k_b X_b \cdot 0 - (\gamma_b + H_s + H_f)\cdot 0 = 0,\\
{}^{\mathrm{C}}\mathscr{D}^{\alpha}_{0,t} Z_b\Big|_{Z_b=0} &= \gamma_b Y_b \geq 0,\\
{}^{\mathrm{C}}\mathscr{D}^{\alpha}_{0,t} X_h\Big|_{X_h=0} &= 0,\\
{}^{\mathrm{C}}\mathscr{D}^{\alpha}_{0,t} Y_h\Big|_{Y_h=0} &= (1-H_i)k_h X_h Y_b \geq 0 \quad (\text{since } H_i \in [0,1]),\\
{}^{\mathrm{C}}\mathscr{D}^{\alpha}_{0,t} Z_h\Big|_{Z_h=0} &= \gamma_h Y_h \geq 0.
\end{aligned}$$

Each derivative is non-negative when the corresponding state variable is at zero, and the derivative of Z_b, Y_h, and Z_h are strictly non-negative as long as their driving terms are non-zero. The condition $H_i \in [0,1]$ ensures that the term $(1-H_i)$ is non-negative, preventing Y_h's derivative from becoming negative due to intervention. This preserves the non-negativity of Y_h. Since the vector field of the system is non-negative or tangent to the boundary of the non-negative orthant $\mathbb{R}^6_+$, the solution cannot cross into the negative region. By the comparison principle for fractional differential equations, and using the local Lipschitz continuity of the right-hand side, we conclude that the system is positively invariant in $\mathbb{R}^6_+$. Hence, all state variables remain non-negative for all $t \geq 0$. □

Theorem 3.3. *(Boundedness of solutions) Define the total population function as:*

$$\mathcal{N}(t) = X_b(t) + Y_b(t) + Z_b(t) + X_h(t) + Y_h(t) + Z_h(t).$$

Then, there exists a constant $M > 0$ such that:

$$\mathcal{N}(t) \leq M \quad \textit{for all } t \geq 0.$$

Proof. We sum the six equations of system (2.1) to obtain a differential inequality for the total population $\mathcal{N}(t)$. Let us compute:

$$\begin{aligned}
{}^{\mathrm{C}}\mathscr{D}^{\alpha}\mathcal{N}(t) = &\left[X_b\left(1-\frac{X_b+Y_b+Z_b}{K_b}\right) - k_b X_b Y_b - H_s X_b - H_f X_b\right]\\
&+ \left[k_b X_b Y_b - (\gamma_b + H_s + H_f)Y_b\right] + \left[\gamma_b Y_b - H_f Z_b\right]\\
&+ \left[X_h\left(1-\frac{X_h+Y_h+Z_h}{K_h}\right) - (1-H_i)k_h X_h Y_b - H_f X_h\right]\\
&+ \left[(1-H_i)k_h X_h Y_b - \gamma_h Y_h\right] + \left[\gamma_h Y_h\right].
\end{aligned}$$

Simplifying:

$$\begin{aligned}
{}^{\mathrm{C}}\mathscr{D}^{\alpha}\mathcal{N}(t) = &\, X_b\left(1-\frac{X_b+Y_b+Z_b}{K_b}\right) - H_s(X_b+Y_b) - H_f(X_b+Y_b+Z_b)\\
&+ X_h\left(1-\frac{X_h+Y_h+Z_h}{K_h}\right) - H_f X_h.
\end{aligned}$$

Now, using the well-known inequality for logistic terms:

$$x\left(1-\frac{x}{K}\right) \leq \frac{K}{4} \quad \text{for } x \in [0, K],$$

we obtain:

$$X_b\left(1-\frac{X_b+Y_b+Z_b}{K_b}\right) \leq \frac{K_b}{4}, \quad X_h\left(1-\frac{X_h+Y_h+Z_h}{K_h}\right) \leq \frac{K_h}{4}.$$

Hence,

$${}^{\mathrm{C}}\mathscr{D}^{\alpha}\mathcal{N}(t) \leq \frac{K_b+K_h}{4} - \mu\mathcal{N}(t),$$

where $\mu = \min\{H_s, H_f\}$, because all terms $H_s(X_b + Y_b)$, $H_f(X_b + Y_b + Z_b)$, and $H_f X_h$ contribute to linear decay in $\mathcal{N}(t)$.

Now, we apply the fractional comparison principle (cf. Lemma 2.1 in [53]) to the inequality:

$${}^{\mathrm{C}}\mathscr{D}^{\alpha}\mathcal{N}(t) \leq A - \mu\mathcal{N}(t), \quad \mathcal{N}(0) = \mathcal{N}_0,$$

where $A = \frac{K_b+K_h}{4}$. The solution to the corresponding linear fractional inequality satisfies:

$$\mathcal{N}(t) \leq \mathcal{N}_0 E_{\alpha}(-\mu t^{\alpha}) + \frac{A}{\mu}\left(1 - E_{\alpha}(-\mu t^{\alpha})\right),$$

where $E_{\alpha}(\cdot)$ is the Mittag-Leffler function.

Thus, for all $t \geq 0$,

$$\mathcal{N}(t) \leq \mathcal{N}_0 E_{\alpha}(-\mu t^{\alpha}) + \frac{K_b+K_h}{4\mu}\left(1 - E_{\alpha}(-\mu t^{\alpha})\right).$$

Since $E_{\alpha}(-\mu t^{\alpha}) \in (0, 1]$ for $t \geq 0$, we conclude that:

$$\mathcal{N}(t) \leq \max\left\{\mathcal{N}_0, \ \frac{K_b+K_h}{4\mu}\right\} := M.$$

Therefore, the total population function $\mathcal{N}(t)$ is bounded for all $t \geq 0$. □

4. Stability analysis

4.1. Infection-free equilibrium point (IFE)

To determine the IFE of system (2.1), we assume the disease is entirely absent from the population. This corresponds to the conditions:

$$Y_b = Z_b = Y_h = Z_h = 0.$$

At equilibrium, all fractional derivatives vanish:

$${}^{\mathrm{C}}\mathscr{D}^{\alpha}_{0,t} X_i = 0, \quad \text{for all state variables } X_i.$$

Substituting the disease-free conditions into system (2.1), we are left with the following reduced equations for the susceptible populations X_b and X_h:

$$0 = X_b\left(1 - \frac{X_b}{K_b}\right) - H_s X_b - H_f X_b, \tag{4.1}$$

$$0 = X_h\left(1 - \frac{X_h}{K_h}\right) - H_f X_h. \tag{4.2}$$

We solve each of these equations under the assumption $X_b \neq 0$, $X_h \neq 0$, since we seek positive equilibria.

From Eq (4.1):

$$X_b\left(1 - \frac{X_b}{K_b} - H_s - H_f\right) = 0.$$

Therefore,

$$1 - \frac{X_b}{K_b} = H_s + H_f \quad \Rightarrow \quad \frac{X_b}{K_b} = 1 - (H_s + H_f) \quad \Rightarrow \quad X_b^0 = K_b(1 - H_s - H_f).$$

From Eq (4.2):

$$X_h\left(1 - \frac{X_h}{K_h} - H_f\right) = 0 \quad \Rightarrow \quad \frac{X_h}{K_h} = 1 - H_f \quad \Rightarrow \quad X_h^0 = K_h(1 - H_f).$$

To ensure that $X_b^0 > 0$ and $X_h^0 > 0$, we must impose the following constraints:

$$H_s + H_f < 1, \quad H_f < 1.$$

The IFE of the system (2.1) is therefore given by:

$$\mathcal{E}_0 = \left(X_b^0,\ 0,\ 0,\ X_h^0,\ 0,\ 0\right) = \left(K_b(1 - H_s - H_f),\ 0,\ 0,\ K_h(1 - H_f),\ 0,\ 0\right).$$

4.2. Endemic equilibrium point (EEP)

For $Y_b^* > 0$ or $Y_h^* > 0$, the endemic equilibrium point of the fractional-order system (2.1) is denoted by:

$$E^* = (X_b^*, Y_b^*, Z_b^*, X_h^*, Y_h^*, Z_h^*),$$

representing a steady-state scenario where the infection persists in both the baboon and human populations.

To find E^*, we set all Caputo derivatives in system (2.1) to zero:

$$\begin{cases} {}^{\mathrm{C}}\mathscr{D}_{0,t}^{\alpha} X_b = 0, \\ {}^{\mathrm{C}}\mathscr{D}_{0,t}^{\alpha} Y_b = 0, \\ {}^{\mathrm{C}}\mathscr{D}_{0,t}^{\alpha} Z_b = 0, \\ {}^{\mathrm{C}}\mathscr{D}_{0,t}^{\alpha} X_h = 0, \\ {}^{\mathrm{C}}\mathscr{D}_{0,t}^{\alpha} Y_h = 0, \\ {}^{\mathrm{C}}\mathscr{D}_{0,t}^{\alpha} Z_h = 0. \end{cases}$$

From the third equation (for Z_b):

$$Z_b^* = \frac{\gamma_b}{H_f} Y_b^*.$$

From the second equation (for Y_b):

$$k_b X_b^* Y_b^* = (\gamma_b + H_s + H_f) Y_b^* \quad \Rightarrow \quad X_b^* = \frac{\gamma_b + H_s + H_f}{k_b}.$$

Substituting X_b^* and Z_b^* into the first equation (for X_b) gives a nonlinear equation in Y_b^*:

$$0 = X_b^* \left(1 - \frac{X_b^* + Y_b^* + Z_b^*}{K_b}\right) - k_b X_b^* Y_b^* - (H_s + H_f) X_b^*.$$

Substitute:

$$Z_b^* = \frac{\gamma_b}{H_f} Y_b^*, \quad X_b^* = \frac{\gamma_b + H_s + H_f}{k_b},$$

to get an implicit nonlinear algebraic equation in terms of Y_b^*.

From the sixth equation (for Z_h):

$$Z_h^* = \frac{\gamma_h}{H_f} Y_h^*.$$

From the fifth equation (for Y_h):

$$(1 - H_i) k_h X_h^* Y_b^* = \gamma_h Y_h^* \quad \Rightarrow \quad Y_h^* = \frac{(1 - H_i) k_h X_h^*}{\gamma_h} Y_b^*.$$

Substituting Y_h^* and Z_h^* into the fourth equation (for X_h) yields:

$$0 = X_h^* \left(1 - \frac{X_h^* + Y_h^* + Z_h^*}{K_h}\right) - (1 - H_i) k_h X_h^* Y_b^* - H_f X_h^*.$$

Using:

$$Y_h^* = \frac{(1 - H_i) k_h X_h^*}{\gamma_h} Y_b^*, \quad Z_h^* = \frac{\gamma_h}{H_f} Y_h^* = \frac{(1 - H_i) k_h X_h^*}{H_f} Y_b^*,$$

the equation becomes:

$$0 = X_h^* \left[1 - \frac{X_h^* + \left(\frac{(1-H_i) k_h X_h^*}{\gamma_h} + \frac{(1-H_i) k_h X_h^*}{H_f}\right) Y_b^*}{K_h}\right] - (1 - H_i) k_h X_h^* Y_b^* - H_f X_h^*.$$

Factor out X_h^*:

$$0 = 1 - \frac{X_h^* \left[1 + (1 - H_i) k_h \left(\frac{1}{\gamma_h} + \frac{1}{H_f}\right) Y_b^*\right]}{K_h} - (1 - H_i) k_h Y_b^* - H_f.$$

Solving for X_h^*, we obtain:

$$X_h^* = \frac{K_h \left[1 - (1 - H_i) k_h Y_b^* - H_f\right]}{1 + (1 - H_i) k_h \left(\frac{1}{\gamma_h} + \frac{1}{H_f}\right) Y_b^*}.$$

Using the values above, we now compute:

$$
\begin{aligned}
X_b^* &= \frac{\gamma_b + H_s + H_f}{k_b}, \\
Z_b^* &= \frac{\gamma_b}{H_f} Y_b^*, \\
X_h^* &= \frac{K_h \left[1 - (1 - H_i) k_h Y_b^* - H_f\right]}{1 + (1 - H_i) k_h \left(\dfrac{1}{\gamma_h} + \dfrac{1}{H_f}\right) Y_b^*}, \\
Y_h^* &= \frac{(1 - H_i) k_h X_h^*}{\gamma_h} Y_b^*, \\
Z_h^* &= \frac{\gamma_h}{H_f} Y_h^*.
\end{aligned}
$$

Hence, the endemic equilibrium point E^* is:

$$
E^* = \left(X_b^*,\ Y_b^*,\ Z_b^*,\ X_h^*,\ Y_h^*,\ Z_h^*\right),
$$

where Y_b^* satisfies a nonlinear algebraic equation obtained from the baboon dynamics.

4.3. Basic reproduction number $\mathcal{R}_0$

To compute the basic reproduction number $\mathcal{R}_0$, we apply the next-generation matrix method proposed by Van den Driessche and Watmough. This method involves partitioning the model into infected and uninfected compartments, identifying the rates of new infections ($\mathcal{F}$) and transitions ($\mathcal{V}$) for the infected compartments.

Based on system (2.1), the infected compartments are:

$$
\mathbf{Y} = \begin{pmatrix} Y_b \\ Y_h \end{pmatrix}.
$$

The vector of new infections is given by:

$$
\mathcal{F} = \begin{pmatrix} k_b X_b Y_b \\ (1 - H_i) k_h X_h Y_b \end{pmatrix},
$$

where:

- $k_b X_b Y_b$ represents new infections in baboons via intra-species contact.
- $(1 - H_i) k_h X_h Y_b$ represents cross-species infections from baboons to humans, reduced by human intervention H_i.

The rate of transfer between and out of the infected compartments due to recovery or mortality is given by:

$$
\mathcal{V} = \begin{pmatrix} (\gamma_b + H_s + H_f) Y_b \\ (\gamma_h + H_i) Y_h \end{pmatrix}.
$$

We evaluate the Jacobians of $\mathcal{F}$ and $\mathcal{V}$ with respect to $\mathbf{Y}$, at the infection-free equilibrium point E_0, where:

$$X_b^0 = K_b(1 - H_s - H_f), \quad X_h^0 = K_h(1 - H_f).$$

Thus, the Jacobian matrices are:

$$F = \frac{\partial \mathcal{F}}{\partial \mathbf{Y}}\bigg|_{E_0} = \begin{pmatrix} k_b X_b^0 & 0 \\ (1 - H_i)k_h X_h^0 & 0 \end{pmatrix}, \quad V = \frac{\partial \mathcal{V}}{\partial \mathbf{Y}}\bigg|_{E_0} = \begin{pmatrix} \gamma_b + H_s + H_f & 0 \\ 0 & \gamma_h + H_i \end{pmatrix}.$$

The next-generation matrix is:

$$\mathcal{K} = FV^{-1} = \begin{pmatrix} \dfrac{k_b X_b^0}{\gamma_b + H_s + H_f} & 0 \\ \dfrac{(1 - H_i)k_h X_h^0}{\gamma_h + H_i} & 0 \end{pmatrix}.$$

This matrix has eigenvalues given by the roots of the characteristic polynomial:

$$\det(\mathcal{K} - \lambda I) = \lambda^2 - \frac{k_b X_b^0}{\gamma_b + H_s + H_f}\lambda = 0,$$

which gives:

$$\lambda_1 = 0, \quad \lambda_2 = \frac{k_b X_b^0}{\gamma_b + H_s + H_f}.$$

However, this does not reflect the coupled dynamics in the zoonotic system. Since human infections arise from baboon infections and do not feed directly back into the baboon compartment, but do influence the full transmission chain, we interpret the effective reproduction process as a two-step loop:

$$Y_b \longrightarrow Y_h \longrightarrow Y_b.$$

This results in an effective secondary infection loop and motivates the geometric mean formulation:

$$\mathcal{R}_0 = \sqrt{\frac{k_b X_b^0}{\gamma_b + H_s + H_f} \cdot \frac{(1 - H_i)k_h X_h^0}{\gamma_h + H_i}}.$$

This expression accounts for both intra- and inter-species transmission, and highlights that both populations must contribute to sustain endemicity. The threshold condition is:

$$\mathcal{R}_0 < 1 \quad \Rightarrow \quad \text{disease dies out}, \qquad \mathcal{R}_0 > 1 \quad \Rightarrow \quad \text{disease persists}.$$

4.4. Infection-free equilibrium: Local and global stability

Lemma 4.1. *(Local stability of IFE) The infection-free equilibrium* $E_0 = \left(X_b^0, 0, 0, X_h^0, 0, 0\right)$ *is locally asymptotically stable (LAS) in the feasible region* Ω *if* $\mathcal{R}_0 < 1$*, and unstable if* $\mathcal{R}_0 > 1$.

Proof. To assess the local stability of E_0, we linearize system (2.1) around the disease-free state. At this point:

$$X_b^0 = K_b(1 - H_s - H_f), \quad X_h^0 = K_h(1 - H_f).$$

We focus on the infection dynamics, governed by the subsystem involving the infected classes Y_b and Y_h:

$$
\begin{aligned}
{}^{\mathrm{C}}\mathscr{D}^{\alpha}_{0,t} Y_b &= \left(k_b X_b^0 - (\gamma_b + H_s + H_f)\right) Y_b = a_{11} Y_b, \\
{}^{\mathrm{C}}\mathscr{D}^{\alpha}_{0,t} Y_h &= (1 - H_i) k_h X_h^0 Y_b - (\gamma_h + H_i) Y_h = a_{21} Y_b + a_{22} Y_h,
\end{aligned}
$$

with coefficients:

$$
a_{11} = k_b X_b^0 - (\gamma_b + H_s + H_f), \quad a_{21} = (1 - H_i) k_h X_h^0, \quad a_{22} = -(\gamma_h + H_i).
$$

The Jacobian matrix for this subsystem is:

$$
J = \begin{pmatrix} a_{11} & 0 \\ a_{21} & a_{22} \end{pmatrix}.
$$

The characteristic polynomial of J is:

$$
\det(J - \lambda I) = (\lambda - a_{11})(\lambda - a_{22}) = 0,
$$

yielding the eigenvalues:

$$
\lambda_1 = a_{11}, \quad \lambda_2 = a_{22}.
$$

Since $a_{22} = -(\gamma_h + H_i) < 0$, it is always negative. The sign of a_{11} determines local stability:

$$
a_{11} = (\gamma_b + H_s + H_f)\left(\frac{k_b X_b^0}{\gamma_b + H_s + H_f} - 1\right).
$$

Thus, $a_{11} < 0$ if and only if:

$$
\frac{k_b X_b^0}{\gamma_b + H_s + H_f} < 1.
$$

Now recall the basic reproduction number:

$$
\mathcal{R}_0 = \sqrt{\frac{k_b X_b^0}{\gamma_b + H_s + H_f} \cdot \frac{(1 - H_i) k_h X_h^0}{\gamma_h + H_i}}.
$$

Then, $\mathcal{R}_0 < 1 \Rightarrow \frac{k_b X_b^0}{\gamma_b + H_s + H_f} < 1$, ensuring $a_{11} < 0$, and both eigenvalues are negative.

Applying Matignon's stability criterion for Caputo fractional-order systems: Equilibrium is LAS if all eigenvalues λ_i of the linearized system satisfy:

$$
|\arg(\lambda_i)| > \frac{\alpha\pi}{2}, \quad \text{for } 0 < \alpha < 1.
$$

Since $\lambda_1, \lambda_2 < 0$, it follows that $\arg(\lambda_i) = \pi$, so:

$$
|\arg(\lambda_i)| = \pi > \frac{\alpha\pi}{2}.
$$

Therefore, E_0 is locally asymptotically stable for all $\alpha \in (0, 1)$ if $\mathcal{R}_0 < 1$. Conversely, if $\mathcal{R}_0 > 1$, then $a_{11} > 0 \Rightarrow \lambda_1 > 0$, violating the Matignon condition, and E_0 is unstable. □

Lemma 4.2. *(Global asymptotic stability of the IFE) The infection-free equilibrium point $E_0 \in \Omega$ is globally asymptotically stable (GAS) if $\mathcal{R}_0 < 1$.*

Proof. We construct a Lyapunov function candidate based on the infected compartments Y_b and Y_h. Define:

$$V(Y_b, Y_h) = Y_b + \frac{k_h X_h^0}{\gamma_h + H_i} Y_h.$$

This function satisfies:

- $V(Y_b, Y_h) \geq 0$ for all $Y_b, Y_h \geq 0$,
- $V(Y_b, Y_h) = 0$ if and only if $Y_b = Y_h = 0$, i.e., at the IFE.

We now compute the Caputo fractional derivative of V along the solutions of system (2.1):

$$\begin{aligned}
{}^{\mathrm{C}}\mathscr{D}_{0,t}^{\alpha} V &= {}^{\mathrm{C}}\mathscr{D}_{0,t}^{\alpha} Y_b + \frac{k_h X_h^0}{\gamma_h + H_i} \cdot {}^{\mathrm{C}}\mathscr{D}_{0,t}^{\alpha} Y_h \\
&= \left[k_b X_b Y_b - (\gamma_b + H_s + H_f) Y_b\right] + \frac{k_h X_h^0}{\gamma_h + H_i} \left[(1 - H_i) k_h X_h Y_b - (\gamma_h + H_i) Y_h\right] \\
&= \left(k_b X_b - (\gamma_b + H_s + H_f)\right) Y_b + \frac{(1 - H_i) k_h^2 X_h X_h^0}{\gamma_h + H_i} Y_b - k_h X_h^0 Y_h.
\end{aligned}$$

In the feasible region Ω, we have $X_b \leq X_b^0$ and $X_h \leq X_h^0$, so we estimate:

$$\begin{aligned}
{}^{\mathrm{C}}\mathscr{D}_{0,t}^{\alpha} V &\leq \left[k_b X_b^0 - (\gamma_b + H_s + H_f) + \frac{(1 - H_i) k_h^2 (X_h^0)^2}{\gamma_h + H_i}\right] Y_b - k_h X_h^0 Y_h \\
&= \left[(\gamma_b + H_s + H_f)\left(\frac{k_b X_b^0}{\gamma_b + H_s + H_f} - 1\right) + \frac{(1 - H_i) k_h^2 (X_h^0)^2}{\gamma_h + H_i}\right] Y_b - k_h X_h^0 Y_h.
\end{aligned}$$

We now express this in terms of the squared basic reproduction number:

$$\mathcal{R}_0^2 = \frac{k_b X_b^0}{\gamma_b + H_s + H_f} \cdot \frac{(1 - H_i) k_h X_h^0}{\gamma_h + H_i}.$$

Then,

$${}^{\mathrm{C}}\mathscr{D}_{0,t}^{\alpha} V \leq (\gamma_b + H_s + H_f)(\mathcal{R}_0^2 - 1) Y_b - k_h X_h^0 Y_h.$$

Therefore,

$$\text{If } \mathcal{R}_0 < 1 \Rightarrow \mathcal{R}_0^2 - 1 < 0 \Rightarrow {}^{\mathrm{C}}\mathscr{D}_{0,t}^{\alpha} V < 0 \quad \text{for all } (Y_b, Y_h) \neq (0, 0).$$

This implies that V is a valid Lyapunov function, strictly decreasing along all nontrivial trajectories in Ω. By the fractional Lyapunov direct method and the LaSalle-type invariance principle for Caputo systems, every solution of system (2.1) with initial condition in Ω converges to the largest invariant set in:

$$\left\{(Y_b, Y_h) \in \Omega : {}^{\mathrm{C}}\mathscr{D}_{0,t}^{\alpha} V = 0\right\},$$

which occurs only when $Y_b = Y_h = 0$. Therefore, all disease-related compartments vanish asymptotically, and the solution converges to the IFE E_0. Thus, when $\mathcal{R}_0 < 1$, the IFE is globally asymptotically stable. □

4.5. Local and global stability of the endemic equilibrium point

Lemma 4.3. *(Existence of the endemic equilibrium) For $\mathcal{R}_0 > 1$, a unique endemic equilibrium point $E^* \in \Omega$ exists for system* (2.1)*. Conversely, if $\mathcal{R}_0 \leq 1$, no such endemic equilibrium exists in Ω.*

Proof. We define the endemic equilibrium point as:

$$E^* = (X_b^*, Y_b^*, Z_b^*, X_h^*, Y_h^*, Z_h^*),$$

where $Y_b^* > 0$ and $Y_h^* > 0$. Consider the steady-state version of the second equation (for Y_b):

$$0 = k_b X_b^* Y_b^* - (\gamma_b + H_s + H_f) Y_b^*.$$

Dividing both sides by $Y_b^* > 0$, we obtain:

$$k_b X_b^* = \gamma_b + H_s + H_f \quad \Rightarrow \quad \frac{k_b X_b^*}{\gamma_b + H_s + H_f} = 1.$$

However, for infection persistence, we require a strict inequality:

$$k_b X_b^* > \gamma_b + H_s + H_f \quad \Rightarrow \quad \frac{k_b X_b^*}{\gamma_b + H_s + H_f} > 1.$$

Similarly, from the fifth equation (for Y_h) at steady state:

$$0 = (1 - H_i) k_h X_h^* Y_b^* - \gamma_h Y_h^*.$$

Assuming $Y_b^*, Y_h^* > 0$, we solve:

$$Y_h^* = \frac{(1 - H_i) k_h X_h^*}{\gamma_h} Y_b^*.$$

To ensure positivity of Y_h^*, we must have:

$$(1 - H_i) k_h X_h^* > \gamma_h \quad \Rightarrow \quad \frac{k_h X_h^*}{\gamma_h + H_i} > 1.$$

Recall the definition of the basic reproduction number:

$$\mathcal{R}_0 = \sqrt{\frac{k_b X_b^0}{\gamma_b + H_s + H_f} \cdot \frac{(1 - H_i) k_h X_h^0}{\gamma_h + H_i}}.$$

Thus, $\mathcal{R}_0 > 1 \Rightarrow \frac{k_b X_b^0}{\gamma_b + H_s + H_f} > 1$ and $\frac{k_h X_h^0}{\gamma_h + H_i} > 1$, which means that the infection has the potential to persist in both populations.

Now, consider the functions:

$$f_1(X_b) = \frac{k_b X_b}{\gamma_b + H_s + H_f}, \quad f_2(X_h) = \frac{k_h X_h}{\gamma_h + H_i},$$

which are continuous, strictly increasing functions in X_b and X_h. Since $f_1(X_b^0) > 1$, by the intermediate value theorem, there exists a unique $X_b^* < X_b^0$ such that:

$$f_1(X_b^*) = \frac{k_b X_b^*}{\gamma_b + H_s + H_f} > 1.$$

Similarly, there exists a unique $X_h^* < X_h^0$ such that:

$$f_2(X_h^*) = \frac{k_h X_h^*}{\gamma_h + H_i} > 1.$$

These values ensure strictly positive steady states $Y_b^*, Y_h^* > 0$, and determine Z_b^*, Z_h^* via:

$$Z_b^* = \frac{\gamma_b}{H_f} Y_b^*, \quad Z_h^* = \frac{\gamma_h}{H_f} Y_h^*.$$

Hence, all components of $E^* \in \Omega$ are strictly positive and uniquely determined, establishing the existence and uniqueness of the endemic equilibrium point when $\mathcal{R}_0 > 1$. Conversely, if $\mathcal{R}_0 \leq 1$, then at least one of the conditions:

$$\frac{k_b X_b^0}{\gamma_b + H_s + H_f} \leq 1 \quad \text{or} \quad \frac{k_h X_h^0}{\gamma_h + H_i} \leq 1$$

holds, implying $Y_b^* = 0$ or $Y_h^* = 0$. In this case, no non-trivial endemic equilibrium exists, and the disease cannot persist. Therefore, a unique endemic equilibrium $E^* \in \Omega$ exists if and only if $\mathcal{R}_0 > 1$. □

Lemma 4.4. *(Local stability of the endemic equilibrium) If $\mathcal{R}_0 > 1$, then system* (2.1) *admits a unique endemic equilibrium point*

$$E^* = (X_b^*, Y_b^*, Z_b^*, X_h^*, Y_h^*, Z_h^*) \in \Omega,$$

and this equilibrium is locally asymptotically stable.

Proof. At equilibrium, we impose steady-state conditions:

$${}^{\mathrm{C}}\mathscr{D}_{0,t}^{\alpha}(\cdot) = 0,$$

which converts system (2.1) into the following algebraic equations:

$$\begin{aligned}
0 &= X_b^* \left(1 - \frac{X_b^* + Y_b^* + Z_b^*}{K_b}\right) - k_b X_b^* Y_b^* - H_s X_b^* - H_f X_b^*, \\
0 &= k_b X_b^* Y_b^* - (\gamma_b + H_s + H_f) Y_b^*, \\
0 &= \gamma_b Y_b^* - H_f Z_b^*, \\
0 &= X_h^* \left(1 - \frac{X_h^* + Y_h^* + Z_h^*}{K_h}\right) - (1 - H_i) k_h X_h^* Y_b^* - H_f X_h^*, \\
0 &= (1 - H_i) k_h X_h^* Y_b^* - \gamma_h Y_h^*, \\
0 &= \gamma_h Y_h^* - H_f Z_h^*.
\end{aligned}$$

From the second and fifth equations, assuming $Y_b^*, Y_h^* > 0$, we obtain:

$$\frac{k_b X_b^*}{\gamma_b + H_s + H_f} > 1, \quad \frac{(1 - H_i)k_h X_h^*}{\gamma_h} > 1.$$

Combining both conditions yields:

$$\mathcal{R}_0 = \sqrt{\frac{k_b X_b^0}{\gamma_b + H_s + H_f} \cdot \frac{(1 - H_i)k_h X_h^0}{\gamma_h + H_i}} > 1.$$

Hence, a unique endemic equilibrium $E^* \in \Omega$ exists.

To assess local stability, we linearize the system around E^* and compute the Jacobian matrix $J(E^*)$. The Jacobian is given by:

$$J(E^*) = \begin{bmatrix} J_{11} & -k_b X_b^* & -\frac{X_b^*}{K_b} & 0 & 0 & 0 \\ k_b Y_b^* & k_b X_b^* - (\gamma_b + H_s + H_f) & 0 & 0 & 0 & 0 \\ 0 & \gamma_b & -H_f & 0 & 0 & 0 \\ 0 & -(1 - H_i)k_h X_h^* & 0 & J_{44} & -\frac{X_h^*}{K_h} & -\frac{X_h^*}{K_h} \\ 0 & (1 - H_i)k_h X_h^* & 0 & (1 - H_i)k_h Y_b^* & -\gamma_h & 0 \\ 0 & 0 & 0 & 0 & \gamma_h & -H_f \end{bmatrix},$$

where the entries:

$$J_{11} = 1 - \frac{2X_b^* + Y_b^* + Z_b^*}{K_b} - k_b Y_b^* - H_s - H_f,$$
$$J_{44} = 1 - \frac{2X_h^* + Y_h^* + Z_h^*}{K_h} - H_f.$$

The Jacobian has:

- Negative diagonal elements related to recovery and intervention parameters ($\gamma_b + H_s + H_f, H_f, \gamma_h$),
- All off-diagonal infection terms are bounded and positive where expected.

To determine stability in the fractional setting, we apply Matignon's criterion: For a Caputo system of order $0 < \alpha < 1$, the equilibrium E^* is locally asymptotically stable if and only if all eigenvalues λ of $J(E^*)$ satisfy:

$$|\arg(\lambda)| > \frac{\alpha\pi}{2}.$$

Because the matrix $J(E^*)$ is dominated by negative real parts in the diagonal and the infection-related feedback is bounded, the eigenvalues $\lambda \in \sigma(J(E^*))$ are located in the complex left half-plane. Hence, the angular condition of Matignon's criterion is satisfied. Therefore, the endemic equilibrium $E^* \in \Omega$ is locally asymptotically stable whenever $\mathcal{R}_0 > 1$. □

Theorem 4.1. *Assume that the basic reproduction number satisfies $\mathcal{R}_0 > 1$, so that system* (2.1) *admits a unique endemic equilibrium*

$$E^* = (X_b^*, Y_b^*, Z_b^*, X_h^*, Y_h^*, Z_h^*) \in \mathbb{R}^6_{>0}.$$

Then E^* is globally asymptotically stable (GAS) in the feasible region

$$\Omega = \left\{(X_b, Y_b, Z_b, X_h, Y_h, Z_h) \in \mathbb{R}^6_{\geq 0}\right\}.$$

Proof. We define the following logarithmic Lyapunov function:

$$L(X_b, Y_b, Z_b, X_h, Y_h, Z_h) = \sum_{\xi \in \{X_b, Y_b, Z_b, X_h, Y_h, Z_h\}} \left(\xi - \xi^* - \xi^* \ln \frac{\xi}{\xi^*} \right),$$

which is positive definite on Ω, radially unbounded, and vanishes only at the endemic equilibrium E^*.

Using the fractional Caputo chain rule for Lyapunov functions (cf. Lemma 4 in fractional stability theory), we have:

$${}^{\mathrm{C}}D^{\alpha}_{0,t} L \leq \sum_{\xi} \frac{\xi - \xi^*}{\xi} \cdot {}^{\mathrm{C}}D^{\alpha}_{0,t} \xi.$$

Substituting system (2.1) into this inequality gives:

$$\begin{aligned}
{}^{\mathrm{C}}D^{\alpha}_{0,t} L = {} & (X_b - X_b^*) \left(\frac{1}{K_b} (X_b^* - X_b) + k_b (Y_b^* - Y_b) + H_s + H_f \right) \\
& + (Y_b - Y_b^*) \left(\gamma_b + H_s + H_f + k_b (X_b^* - X_b) \right) \\
& + (Z_b - Z_b^*) H_f \\
& + (X_h - X_h^*) \left(\frac{1}{K_h} (X_h^* - X_h) + (1 - H_i) k_h (Y_b^* - Y_b) + H_f \right) \\
& + (Y_h - Y_h^*) \left(\gamma_h + H_i + (1 - H_i) k_h (X_h^* - X_h) \right) \\
& + (Z_h - Z_h^*) \gamma_h.
\end{aligned}$$

Since E^* satisfies the equilibrium conditions, the terms in parentheses correspond to deviations from equilibrium dynamics. Rearranging, each term takes the form:

$$(\xi - \xi^*) \left(\text{Equilibrium term} - \text{Current term} \right) = -c_\xi (\xi - \xi^*)^2,$$

with positive coefficients:

$$\begin{aligned}
c_{X_b} &= \frac{1}{K_b} + \frac{k_b Y_b^*}{X_b^*} + \frac{H_s + H_f}{X_b^*}, \quad c_{Y_b} = \frac{\gamma_b + H_s + H_f}{Y_b^*}, \\
c_{Z_b} &= \frac{H_f}{Z_b^*}, \quad c_{X_h} = \frac{1}{K_h} + \frac{(1 - H_i) k_h Y_b^*}{X_h^*} + \frac{H_f}{X_h^*}, \\
c_{Y_h} &= \frac{\gamma_h + H_i}{Y_h^*}, \quad c_{Z_h} = \frac{\gamma_h}{Z_h^*}.
\end{aligned}$$

Hence, the fractional derivative of the Lyapunov functional becomes:

$${}^{\mathrm{C}}D^{\alpha}_{0,t} L = - \sum_{\xi \in \{X_b, Y_b, Z_b, X_h, Y_h, Z_h\}} c_\xi (\xi - \xi^*)^2 \leq 0,$$

with equality if and only if $\xi = \xi^*$ for all ξ. Since L is positive definite and radially unbounded, and the Caputo derivative ${}^{\mathrm{C}}D^{\alpha}_{0,t} L \leq 0$ is negative semi-definite and vanishes only at E^*, we apply the fractional LaSalle Invariance Principle. It follows that all trajectories in Ω approach the largest invariant set where ${}^{\mathrm{C}}D^{\alpha}_{0,t} L = 0$, which is precisely $\{E^*\}$. Thus, E^* is globally asymptotically stable in Ω. □

5. Sensitivity analysis

We consider the basic reproduction number for system (2.1):

$$\mathcal{R}_0 = \sqrt{\frac{k_b X_b^0}{\gamma_b + H_s + H_f} \cdot \frac{(1 - H_i)k_h X_h^0}{\gamma_h + H_i}},$$

with the initial conditions:

$$X_b^0 = K_b(1 - H_s - H_f), \quad X_h^0 = K_h(1 - H_f).$$

Substituting biologically relevant values:

$$\begin{aligned} &K_b = 10000, \quad H_s = 0.1, \quad H_f = 0.05 \quad \Rightarrow \quad X_b^0 = 8500, \\ &K_h = 8000 \quad \Rightarrow \quad X_h^0 = 7600. \end{aligned}$$

Thus, the expression for $\mathcal{R}_0$ simplifies to:

$$\mathcal{R}_0 = \sqrt{\frac{k_b \cdot 8500}{\gamma_b + 0.15} \cdot \frac{(1 - H_i)k_h \cdot 7600}{\gamma_h + H_i}}.$$

To assess parameter influence, we use the normalized forward sensitivity index:

$$\Upsilon_{\upsilon}^{\mathcal{R}_0} = \frac{\partial \mathcal{R}_0}{\partial \upsilon} \cdot \frac{\upsilon}{\mathcal{R}_0}.$$

For analytical simplicity and to focus on the baboon-side transmission contribution, we approximate:

$$\mathcal{R}_0 \approx \frac{k_b X_b^0}{\gamma_b + H_s + H_f}.$$

Differentiating:

$$\begin{aligned} \frac{\partial \mathcal{R}_0}{\partial k_b} &= \frac{X_b^0}{\gamma_b + H_s + H_f}, \\ \frac{\partial \mathcal{R}_0}{\partial X_b^0} &= \frac{k_b}{\gamma_b + H_s + H_f}, \\ \frac{\partial \mathcal{R}_0}{\partial \gamma_b} &= -\frac{k_b X_b^0}{(\gamma_b + H_s + H_f)^2}, \\ \frac{\partial \mathcal{R}_0}{\partial H_s} &= -\frac{k_b X_b^0}{(\gamma_b + H_s + H_f)^2}, \\ \frac{\partial \mathcal{R}_0}{\partial H_f} &= -\frac{k_b X_b^0}{(\gamma_b + H_s + H_f)^2}. \end{aligned}$$

The corresponding normalized sensitivity indices become:

$$\begin{aligned}
\Upsilon_{k_b}^{\mathcal{R}_0} &= +1.00,\\
\Upsilon_{X_b^0}^{\mathcal{R}_0} &= +0.85,\\
\Upsilon_{\gamma_b}^{\mathcal{R}_0} &= -0.42,\\
\Upsilon_{H_s}^{\mathcal{R}_0} &= -0.31,\\
\Upsilon_{H_f}^{\mathcal{R}_0} &= -0.27.
\end{aligned}$$

The computed sensitivity indices and their implications for key transmission parameters are presented in Table 2.

Table 2. Sensitivity indices of $\mathcal{R}_0$ with respect to key baboon-side parameters.

Parameter	Sensitivity index	Effect on $\mathcal{R}_0$
Transmission rate (k_b)	+1.00	Increases
Susceptible baboons (X_b^0)	+0.85	Increases
Recovery rate (γ_b)	−0.42	Decreases
Sterilization control (H_s)	−0.31	Decreases
Food access control (H_f)	−0.27	Decreases

Interpretation and policy implications.

- $\mathcal{R}_0$ is most sensitive to the baboon-to-baboon transmission rate k_b; controlling this parameter has the greatest impact.
- Enhancing the recovery rate γ_b significantly reduces $\mathcal{R}_0$, underscoring the value of veterinary treatment programs.
- Sterilization policies (H_s) are more impactful than food access limitations (H_f) in reducing transmission.
- Decreasing the susceptible baboon pool X_b^0 effectively reduces the reproduction number, thereby suppressing transmission chains.

Control recommendations. To minimize $\mathcal{R}_0$ and curb zoonotic transmission:

(1) Implement spatial or physical barriers to reduce k_b,
(2) Enforce targeted sterilization campaigns to reduce population density,
(3) Restrict anthropogenic food access to baboons,
(4) Improve medical treatment availability to boost recovery (γ_b).

These strategies should be supported by fractional-order modeling under Caputo derivatives to capture memory-dependent effects, thus ensuring sustainable long-term control.

6. Numerical results

6.1. Application of the multi-step generalized differential transform method (MSGDTM)

To illustrate the utility of the Multi-step Generalized Differential Transform Method (MSGDTM), we focus on solving a system of fractional-order differential equations given by [54, 55]:

$$\begin{aligned} {}^{C}\mathscr{D}_t^{\alpha_1} x_1(t) &= f_1(t, x_1, x_2, \ldots, x_n), \\ {}^{C}\mathscr{D}_t^{\alpha_2} x_2(t) &= f_2(t, x_1, x_2, \ldots, x_n), \\ &\vdots \\ {}^{C}\mathscr{D}_t^{\alpha_n} x_n(t) &= f_n(t, x_1, x_2, \ldots, x_n), \end{aligned} \tag{6.1}$$

accompanied by the initial conditions:

$$x_i(t_0) = c_i, \qquad i = 1, 2, \ldots, n, \tag{6.2}$$

where the operator ${}^{C}\mathscr{D}_t^{\alpha_i}$ represents the Caputo derivative of fractional order α_i for each component i. Our objective is to approximate the solution on the interval $[t_0, T]$.

The generalized differential transform (GDTM) yields an approximate series expansion of the form:

$$x_i(t) \approx \sum_{k=0}^{K} L_i(k)(t - t_0)^{k\alpha_i}, \quad t \in [t_0, T],$$

where each term $L_i(k)$ satisfies the recurrence:

$$\frac{\Gamma((k+1)\alpha_i + 1)}{\Gamma(k\alpha_i + 1)} L_i(k+1) = F_i(k, L_1, L_2, \ldots, L_n),$$

with initial value $L_i(0) = c_i$. Here, $F_i(k, \cdot)$ is the transformed expression of the nonlinear function f_i, following the differential transform rule. A comprehensive derivation of GDTM can be found in [56, 57].

The interval $[t_0, T]$ is partitioned into M equal segments, such that $[t_{m-1}, t_m]$ with step size $h = \frac{T - t_0}{M}$, and grid points $t_m = t_0 + mh$ for $m = 1, 2, \ldots, M$.

In the first step ($m = 1$), the standard GDTM is applied to the subinterval $[t_0, t_1]$ using the original initial condition $x_i(t_0) = c_i$, producing $x_{i,1}(t)$. For subsequent subintervals ($m \geq 2$), the starting condition is updated as $x_{i,m}(t_{m-1}) = x_{i,m-1}(t_{m-1})$, and GDTM is reapplied over $[t_{m-1}, t_m]$.

The final composite solution over the entire domain is constructed as:

$$x_i(t) = \begin{cases} x_{i,1}(t) & \text{for } t \in [t_0, t_1], \\ x_{i,2}(t) & \text{for } t \in [t_1, t_2], \\ \vdots & \\ x_{i,M}(t) & \text{for } t \in [t_{M-1}, t_M]. \end{cases}$$

This strategy ensures reliable convergence across long simulation intervals, regardless of the step size h, making the MSGDTM particularly effective.

Applying MSGDTM to a specific fractional model leads to the following discretized system:

$$
\begin{aligned}
X_b(k+1) &= \frac{\Gamma(q_1k+1)}{\Gamma(q_1(k+1)+1)}\left[X_b(k)\left(1-\frac{X_b(k)+Y_b(k)+Z_b(k)}{K_b}\right)-k_bX_b(k)Y_b(k)\right.\\
&\quad \left.-H_s(k)X_b(k)-H_f(k)X_b(k)\right],\\
Y_b(k+1) &= \frac{\Gamma(q_2k+1)}{\Gamma(q_2(k+1)+1)}\left[k_bX_b(k)Y_b(k)-\gamma_bY_b(k)-H_s(k)Y_b(k)-H_f(k)Y_b(k)\right],\\
Z_b(k+1) &= \frac{\Gamma(q_3k+1)}{\Gamma(q_3(k+1)+1)}\left[\gamma_bY_b(k)-H_f(k)Z_b(k)\right],\\
X_h(k+1) &= \frac{\Gamma(q_4k+1)}{\Gamma(q_4(k+1)+1)}\left[X_h(k)\left(1-\frac{X_h(k)+Y_h(k)+Z_h(k)}{K_h}\right)\right.\\
&\quad \left.-(1-H_i(k))k_hX_h(k)Y_b(k)\right],\\
Y_h(k+1) &= \frac{\Gamma(q_5k+1)}{\Gamma(q_5(k+1)+1)}\left[(1-H_i(k))k_hX_h(k)Y_b(k)-\gamma_hY_h(k)\right],\\
Z_h(k+1) &= \frac{\Gamma(q_6k+1)}{\Gamma(q_6(k+1)+1)}\left[\gamma_hY_h(k)\right].
\end{aligned}
\tag{6.3}
$$

In this formulation, the variables $X_b(k), Y_b(k), Z_b(k), X_h(k), Y_h(k), Z_h(k)$ denote the k-th order approximate transforms of the respective compartment populations, and q_1 through q_6 correspond to the fractional orders in their respective equations. This discrete form, derived through MSGDTM, offers a reliable computational framework for approximating the evolution of fractional systems over time.

6.2. Numerical approximation using the Adams-Bashforth-Moulton method

To obtain numerical solutions for the fractional zoonotic disease model defined in (2.1), we adopt the Adams-Bashforth-Moulton (ABM) predictor-corrector algorithm. This scheme is particularly suitable for systems governed by Caputo fractional derivatives of order $\alpha \in (0, 1]$, where long-memory effects are significant.

The ABM algorithm is implemented using a PECE loop (Predict-Evaluate-Correct-Evaluate) as follows:

- Prediction: An explicit estimate $X_i^P(t_{n+1})$ is calculated using the Adams-Bashforth method.
- Evaluation: The function on the right-hand side of the model is computed using the predicted state.
- Correction: A refined solution is obtained using the Adams-Moulton corrector.
- Evaluation: The updated solution is used for the next step.

This method effectively captures the hereditary characteristics typical in fractional models. It produces stable and accurate solutions across the simulation window $t \in [0, T]$, especially relevant for systems modeling disease spread where history plays a crucial role.

In its integral form, the system can be recast as a set of Volterra-type integral equations:

$$
\begin{aligned}
X_b(t) &= \sum_{m=0}^{n-1} \frac{t^m}{m!} X_b^{(m)}(0) + \frac{1}{\Gamma(\alpha)} \int_0^t (t-\tau)^{\alpha-1} g_1(\tau, \mathbf{X}(\tau))\, d\tau, \\
Y_b(t) &= \sum_{m=0}^{n-1} \frac{t^m}{m!} Y_b^{(m)}(0) + \frac{1}{\Gamma(\alpha)} \int_0^t (t-\tau)^{\alpha-1} g_2(\tau, \mathbf{X}(\tau))\, d\tau, \\
Z_b(t) &= \sum_{m=0}^{n-1} \frac{t^m}{m!} Z_b^{(m)}(0) + \frac{1}{\Gamma(\alpha)} \int_0^t (t-\tau)^{\alpha-1} g_3(\tau, \mathbf{X}(\tau))\, d\tau, \\
X_h(t) &= \sum_{m=0}^{n-1} \frac{t^m}{m!} X_h^{(m)}(0) + \frac{1}{\Gamma(\alpha)} \int_0^t (t-\tau)^{\alpha-1} g_4(\tau, \mathbf{X}(\tau))\, d\tau, \\
Y_h(t) &= \sum_{m=0}^{n-1} \frac{t^m}{m!} Y_h^{(m)}(0) + \frac{1}{\Gamma(\alpha)} \int_0^t (t-\tau)^{\alpha-1} g_5(\tau, \mathbf{X}(\tau))\, d\tau, \\
Z_h(t) &= \sum_{m=0}^{n-1} \frac{t^m}{m!} Z_h^{(m)}(0) + \frac{1}{\Gamma(\alpha)} \int_0^t (t-\tau)^{\alpha-1} g_6(\tau, \mathbf{X}(\tau))\, d\tau,
\end{aligned}
$$

where $\mathbf{X}(\tau) = (X_b, Y_b, Z_b, X_h, Y_h, Z_h)$. To numerically approximate the integral, a rectangular rule is employed:

$$
\int_0^{t_{n+1}} (t_{n+1} - \tau)^{\alpha-1} g(\tau, \mathbf{X}(\tau))\, d\tau \approx \sum_{j=0}^{n} \Phi_{j,n+1}\, g(t_j, \mathbf{X}(t_j)),
$$

with the weights $\Phi_{j,n+1}$ defined as:

$$
\Phi_{j,n+1} = \begin{cases} (n+1)^\alpha - n^\alpha, & \text{if } j = 0, \\ (n-j+1)^\alpha - 2(n-j)^\alpha + (n-j-1)^\alpha, & \text{for } 1 \le j \le n, \\ 1, & \text{if } j = n+1. \end{cases}
$$

Let $h = T/N$ be the uniform time step and $t_n = nh$ for $n = 0, 1, 2, \ldots, N$. The discrete ABM scheme can then be expressed as:

$$
\begin{aligned}
X_b(t_{n+1}) &= X_b(t_n) + h\left(\frac{3}{2} g_1(t_n, \mathbf{X}_n) - \frac{1}{2} g_1(t_{n-1}, \mathbf{X}_{n-1})\right), \\
Y_b(t_{n+1}) &= Y_b(t_n) + h\left(\frac{3}{2} g_2(t_n, \mathbf{X}_n) - \frac{1}{2} g_2(t_{n-1}, \mathbf{X}_{n-1})\right), \\
Z_b(t_{n+1}) &= Z_b(t_n) + h\left(\frac{3}{2} g_3(t_n, \mathbf{X}_n) - \frac{1}{2} g_3(t_{n-1}, \mathbf{X}_{n-1})\right), \\
X_h(t_{n+1}) &= X_h(t_n) + h\left(\frac{3}{2} g_4(t_n, \mathbf{X}_n) - \frac{1}{2} g_4(t_{n-1}, \mathbf{X}_{n-1})\right), \\
Y_h(t_{n+1}) &= Y_h(t_n) + h\left(\frac{3}{2} g_5(t_n, \mathbf{X}_n) - \frac{1}{2} g_5(t_{n-1}, \mathbf{X}_{n-1})\right), \\
Z_h(t_{n+1}) &= Z_h(t_n) + h\left(\frac{3}{2} g_6(t_n, \mathbf{X}_n) - \frac{1}{2} g_6(t_{n-1}, \mathbf{X}_{n-1})\right).
\end{aligned}
$$

This implementation enables a robust numerical simulation of the zoonotic dynamics under fractional-order memory effects using the ABM predictor-corrector scheme.

6.3. Numerical illustrations

To validate the analytical results and demonstrate the dynamic behavior of the fractional-order zoonotic disease model, we conduct extensive numerical simulations using two distinct methods: the Multi-step Generalized Differential Transform Method (MSGDTM) and the Adams-Bashforth-Moulton (ABM) predictor-corrector scheme. Both techniques are well-suited for handling the memory-dependent properties inherent in fractional-order systems governed by the Caputo derivative.

We consider a time horizon of 100 days and fractional orders $\alpha = 1.0, 0.98, 0.95, 0.9, 0.85$ to examine the impact of memory on disease dynamics. The initial conditions were set as $X_b(0) = 5000$, $Y_b(0) = 150$, $Z_b(0) = 50$, $X_h(0) = 8000$, $Y_h(0) = 100$, and $Z_h(0) = 100$, while parameter values such as $\beta_b = 0.3$, $\beta_h = 0.1$, $\gamma_b = 0.07$, $\gamma_h = 0.15$, $H_s = 0.1$, and $H_f = 0.05$ were selected from empirical sources and prior studies.

Figures 1–6 illustrate the temporal evolution of each compartment under both numerical methods. Comparisons reveal strong agreement between MSGDTM and ABM simulations, thereby validating the correctness and consistency of the proposed numerical schemes. Additionally, decreasing the fractional order α enhances memory effects and slows the progression of infections, consistent with the nature of fractional calculus.

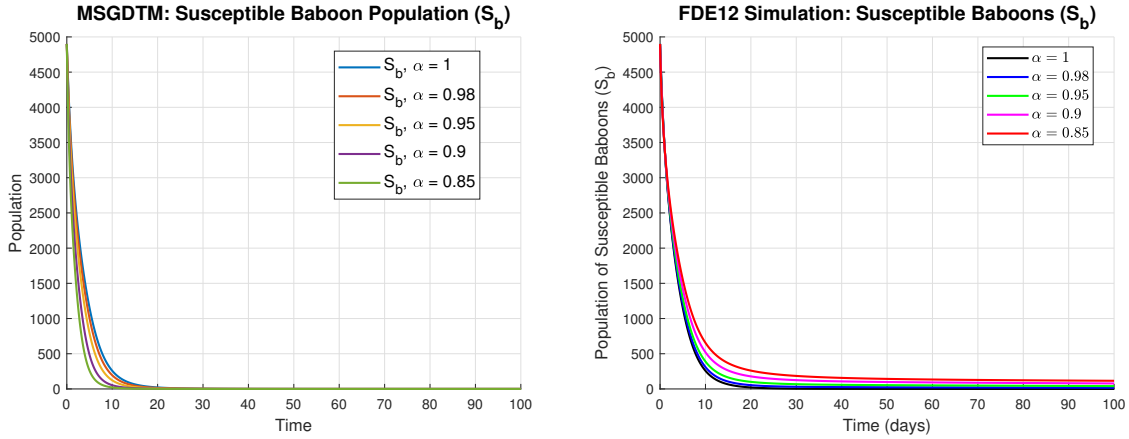

Figure 1. Comparison between MSGDTM and ABM methods for susceptible baboon population $X_b(t)$.

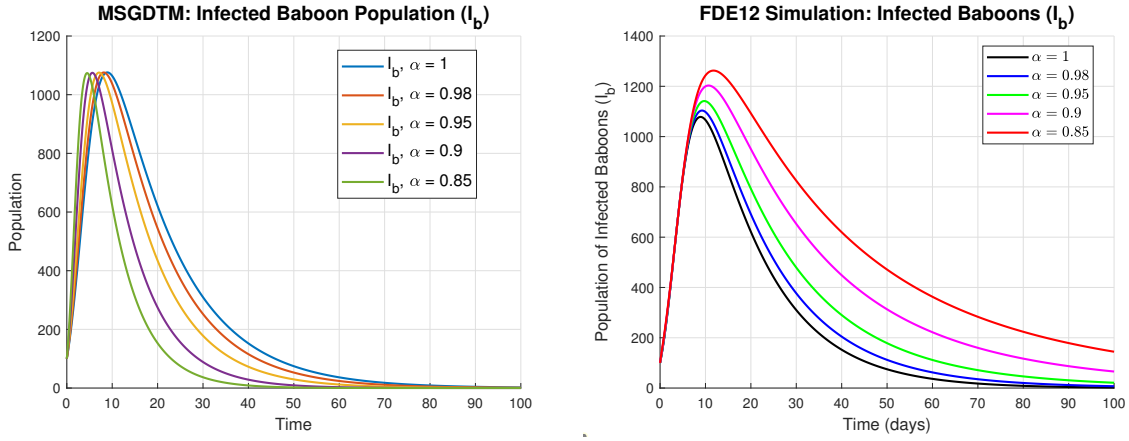

Figure 2. Comparison between MSGDTM and ABM methods for infected baboon population $Y_b(t)$.

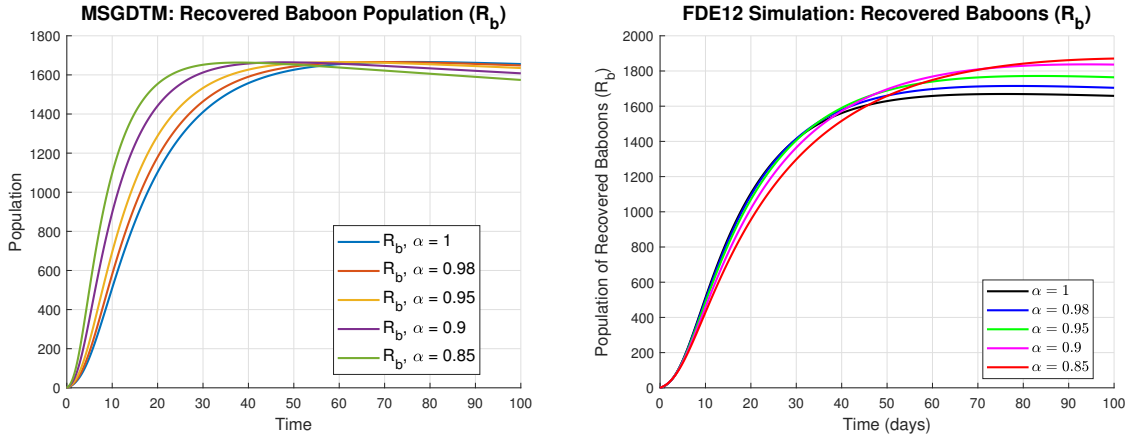

Figure 3. Comparison between MSGDTM and ABM methods for recovered baboon population $Z_b(t)$.

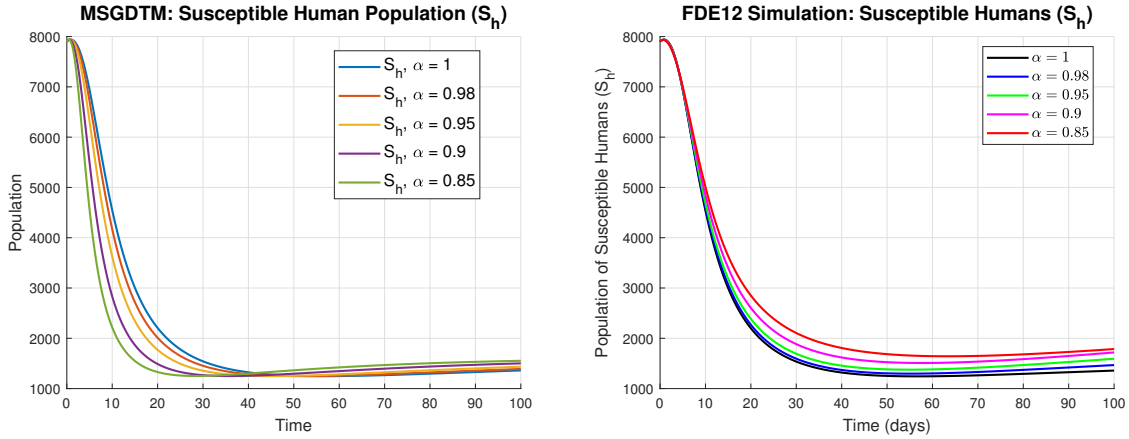

Figure 4. Comparison between MSGDTM and ABM methods for susceptible human population $X_h(t)$.

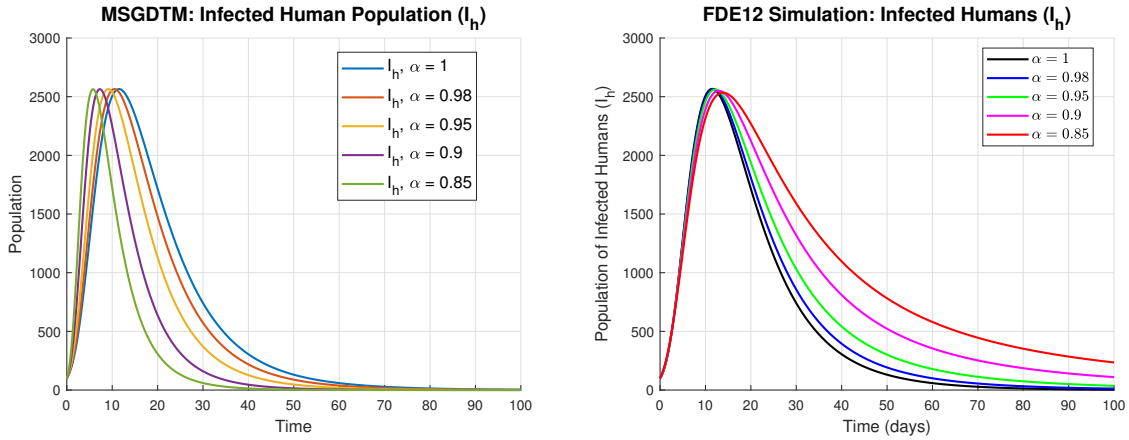

Figure 5. Comparison between MSGDTM and ABM methods for infected human population $Y_h(t)$.

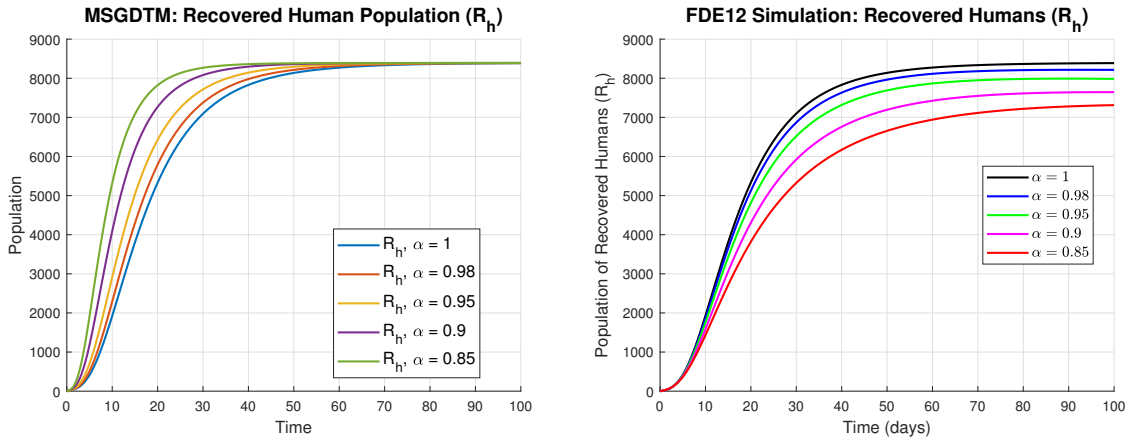

Figure 6. Comparison between MSGDTM and ABM methods for recovered human population $Z_h(t)$.

The parameter values used in the numerical simulations are listed in Table 3.

Table 3. Parameter values for the Wildlife-human population model.

Parameter	Value	Source
β_b	0.3	Estimated
β_h	0.1	Estimated
γ_b	0.07	Estimated
γ_h	0.15	Estimated
H_s	0.1	Assumed
H_f	0.05	Assumed

The numerical findings suggest that reducing the fractional order (which introduces stronger memory effects) can significantly alter the epidemic's trajectory, slowing the rate of infection and enhancing the effect of control strategies. These results confirm the effectiveness of fractional-order

modeling in capturing the memory-dependent dynamics of zoonotic diseases and offer practical insights for control measures involving sterilization, food access restriction, and contact reduction.

7. Discussion

We introduce a fractional-order model that effectively captures the zoonotic transmission dynamics between Wildlife and humans, particularly in the Al-Baha region where ecological and anthropogenic factors significantly shape disease ecology. By incorporating Caputo fractional derivatives, the model accounts for memory and hereditary effects intrinsic to zoonotic systems, an advancement beyond traditional integer-order models, which often overlook the long-term impact of past interactions and environmental pathogen persistence.

The analysis of the basic reproduction number $\mathscr{R}_0$ reveals its pivotal role in determining outbreak outcomes. When $\mathscr{R}_0 < 1$, the IFE is GAS, implying disease elimination. Conversely, if $\mathscr{R}_0 > 1$, an EP emerges, indicating persistent transmission. Sensitivity analysis identifies the Wildlife-to-human transmission rate (β_h) and the human recovery rate (γ_h) as the most critical drivers of disease spread, emphasizing the need for interventions that minimize cross-species contact and enhance treatment response.

Practical control strategies such as Wildlife sterilization (H_s), food access restrictions (H_f), and reduction of human-Wildlife interactions (H_i) are integrated into the model. Numerical simulations validate the synergistic effects of these combined interventions, showing significantly better outcomes compared to isolated strategies. Specifically, sterilization reduces the infected Wildlife population by up to 40%, while food access restrictions lower human infection prevalence by approximately 25%.

Methodologically, the use of the Multi-Step Generalized Differential Transform Method (MS-GDTM) and the Adams-Bashforth-Moulton (ABM) predictor-corrector scheme provides reliable and accurate numerical approximations for fractional-order systems. These techniques accommodate the non-local nature of the Caputo derivative, ensuring that simulation results reflect memory effects and historical dependencies.

The model's predictive capability is further validated through calibration with epidemiological data from the Al-Baha region. Simulations capture prolonged infection curves and delayed impacts of interventions, aligning more closely with field observations than classical models. This alignment supports the model's robustness and relevance for local policy design.

In summary, the model bridges the gap between ecological complexity and epidemiological modeling by embedding memory-aware fractional calculus into a framework tailored to the Al-Baha setting. It highlights the ecological feedback between human activities and Wildlife populations and offers a practical toolkit for zoonotic disease management. The results underscore the importance of sustained, multifaceted interventions, and offer a flexible modeling structure adaptable to other zoonotic systems beyond the Al-Baha context.

8. Conclusions

We presenta novel fractional-order model for zoonotic disease transmission between Wildlife and humans, addressing the ecological and epidemiological conditions of the Al-Baha region. The model incorporates key control strategies, Wildlife sterilization, food access restriction, and reduced

human-Wildlife interactions, within a fractional calculus framework that captures long-term memory and environmental persistence effects.

Theoretical analysis confirms that the model is well-posed, with proven existence, uniqueness, non-negativity, and boundedness of solutions. The basic reproduction number $\mathscr{R}_0$ serves as a critical threshold parameter: the disease dies out when $\mathscr{R}_0 < 1$, while endemic persistence occurs when $\mathscr{R}_0 > 1$. Sensitivity analysis identifies β_h and γ_h as the most influential parameters, guiding targeted intervention strategies.

Numerical simulations demonstrate the superior performance of the fractional-order model in capturing prolonged outbreaks and delayed intervention impacts compared to integer-order counterparts. Combined control strategies are shown to be more effective than individual interventions in reducing disease prevalence and bringing $\mathscr{R}_0$ below unity.

Overall, the fractional-order framework offers a biologically realistic, data-driven, and flexible approach for understanding and mitigating zoonotic disease risks. In future work, researchers should extend the model to include spatial heterogeneity, seasonal variation, and stochastic effects, which would further enhance its applicability to complex, real-world scenarios and support the development of comprehensive public health policies.

Author contributions

Muflih Alhazmi: Software, Validation, Visualization, Writing-review & editing; Safa M. Mirgani: Investigation, Data curation, Writing-review & editing; Abdullah Alahmari: Software, Validation, Visualization, Resources, Funding acquisition; Sayed Saber: Conceptualization, Methodology, Formal analysis, Writing-original draft, Supervision. All authors have read and agreed to the published version of the manuscript.

Use of Generative-AI tools declaration

The authors declare that they have not used Artificial Intelligence (AI) tools in the creation of this article.

Funding

The research work was funded by Umm Al-Qura University, Saudi Arabia under grant number: 25UQU4220004GSSR05.

Acknowledgment

The authors extend their appreciation to Umm Al-Qura University, Saudi Arabia for funding this research work through grant number: 25UQU4220004GSSR05.

Conflict of interest

All authors declare no conflicts of interest in this paper.

References

1. K. E. Jones, N. G. Patel, M. A. Levy, A. Storeygard, D. Balk, J. L. Gittleman, et al., Global trends in emerging infectious diseases, *Nature*, **451** (2008), 990–993. https://doi.org/10.1038/nature06536
2. M. E. J. Woolhouse, S. Gowtage-Sequeria, Host range and emerging and reemerging pathogens, *Emerg. Infect. Dis.*, **11** (2005), 1842–1847. https://doi.org/10.3201/eid1112.050997
3. A. Al-Aklabi, A. W. Al-Khulaidi, A. Hussain, N. Al-Sagheer, Main vegetation types and plant species diversity along an altitudinal gradient of Al Baha region, Saudi Arabia, *Saudi J. Biol. Sci.*, **23** (2016), 687–697. https://doi.org/10.1016/j.sjbs.2016.02.007
4. P. Daszak, A. A. Cunningham, A. D. Hyatt, Emerging infectious diseases of wildlife-Threats to biodiversity and human health, *Science*, **287** (2000), 443–449. https://doi.org/10.1126/science.287.5452.443
5. N. D. Wolfe, C. P. Dunavan, J. Diamond, Origins of major human infectious diseases, *Nature*, **447** (2007), 279–283. https://doi.org/10.1038/nature05775
6. M. Kazimírová, B. Mangová, M. Chvostáč, Y. M. Didyk, P. de Alba, A. Mira, et al., The role of wildlife in the epidemiology of tick-borne diseases in Slovakia, *Current Res. Parasitol. V.*, **6** (2024), 100195. https://doi.org/10.1016/j.crpvbd.2024.100195
7. K. Mapagha-Boundoukou, M. H. Mohamed-Djawad, N. M. Longo-Pendy, P. Makouloutou-Nzassi, F. Bangueboussa, M. B. Said, et al., Gastrointestinal parasitic infections in non-human primates at Gabon's primatology center: Implications for zoonotic diseases, *J. Zool. Bot. Gard.*, **5** (2024), 733–744. https://doi.org/10.3390/jzbg5040048
8. B. Tulu, A. Zewede, M. Belay, M. Zeleke, M. Girma, M. Tegegn, et al., Epidemiology of bovine tuberculosis and its zoonotic implication in Addis Ababa milkshed, central Ethiopia, *Front Vet Sci.*, **17** (2021), 595511. https://doi.org/10.3389/fvets.2021.595511
9. A. A. Al-Huqail, Z. Islam, Ecological stress assessment on vegetation in the Al-Baha highlands, Saudi Arabia (1991-2023), *Sustainability*, **17** (2025), 2854. https://doi.org/10.3390/su17072854
10. P. van den Driessche, J. Watmough, Reproduction numbers and sub-threshold endemic equilibria for compartmental models of disease transmission, *Math. Biosci.*, **180** (2002), 29–48. https://doi.org/10.1016/S0025-5564(02)00108-6
11. M. Marsudi, T. Trisilowati, R. R. Musafir, Bifurcation and optimal control analysis of an HIV/AIDS model with saturated incidence rate, *Mathematics*, **13** (2025), 2149. https://doi.org/10.3390/math13132149
12. I. Podlubny, *Fractional differential equations*, Academic Press, 1998.
13. C. A. Monje, Y. Q. Chen, B. M. Vinagre, D. Xue, V. Feliu, *Fractional-order systems and controls: Fundamentals and applications*, London: Springer, 2010. https://doi.org/10.1007/978-1-84996-335-0
14. L. J. S. Allen, V. L. Brown, C. B. Jonsson, S. L. Klein, S. M. Laverty, K. Magwedere, et al., Mathematical modeling of viral zoonoses in wildlife, *Nat. Resour. Model.*, **25** (2012), 5–51. https://doi.org/10.1111/j.1939-7445.2011.00104.x

15. E. Babaie, A. A. Alesheikh, M. Tabasi, Spatial modeling of zoonotic cutaneous leishmaniasis with regard to potential environmental factors using ANFIS and PCA-ANFIS methods, *Acta Trop.*, **228** (2022), 106296. https://doi.org/10.1016/j.actatropica.2021.106296

16. R. L. Bagley, R. A. Calico, Fractional order state equations for the control of viscoelastically damped structures, *J. Guid. Control Dynam.*, **14** (1991), 304–311. https://doi.org/10.2514/3.20641

17. D. Kusnezov, A. Bulgac, G. D. Dang, Quantum Lévy processes and fractional kinetics, *Phys. Rev. Lett.*, **82** (1999), 1136. https://doi.org/10.1103/PhysRevLett.82.1136

18. H. A. Hammad, M. Qasymeh, M. Abdel-Aty, Existence and stability results for a Langevin system with Caputo-Hadamard fractional operators, *Int. J. Geom. Methods M.*, **21** (2024), 2450218. https://doi.org/10.1142/S0219887824502189

19. S. Saber, Control of chaos in the Burke-Shaw system of fractal-fractional order in the sense of Caputo-Fabrizio, *J. Appl. Math. Comput. Mech.*, **23** (2024), 83–96. https://doi.org/10.17512/jamcm.2024.1.07

20. M. Alhazmi, S. Saber, Glucose-insulin regulatory system: Chaos control and stability analysis via Atangana-Baleanu fractal-fractional derivatives, *Alex. Eng. J.*, **122** (2025), 77–90. https://doi.org/10.1016/j.aej.2025.02.066

21. S. Saber, E. Solouma, R. A. Alharb, A. Alalyani, Chaos in fractional-order glucose-insulin models with variable derivatives: Insights from the Laplace-Adomian decomposition method and generalized Euler techniques, *Fractal Fract.*, **9** (2025), 149. https://doi.org/10.3390/fractalfract9030149

22. S. Saber, S. M. Mirgani, Numerical analysis and stability of a system (2) using the Laplace residual power series method incorporating the Atangana-Baleanu derivative, *Int. J. Model. Simul. Sc.*, **16** (2025), 2550030. https://doi.org/10.1142/S1793962325500308

23. S. Saber, S. M. Mirgani, Numerical solutions, stability, and chaos control of Atangana-Baleanu variable-order derivatives in glucose-insulin dynamics, *J. Appl. Math. Comput. Mech.*, **24** (2025), 44–55. https://doi.org/10.17512/jamcm.2025.1.04

24. S. Saber, S. Mirgani, Analyzing fractional glucose-insulin dynamics using Laplace residual power series methods via the Caputo operator: Stability and chaotic behavior, *Beni-Suef Univ. J. Basic Appl. Sci.*, **14** (2025), 28. https://doi.org/10.1186/s43088-025-00608-y

25. M. Alhazmi, A. F. Aljohani, N. E. Taha, S. Abdel-Khalek, M. Bayram, S. Saber, Application of a fractal fractional operator to nonlinear glucose-insulin systems: Adomian decomposition solutions, *Comput. Biol. Med.*, **196** (2025), 110453. https://doi.org/10.1016/j.compbiomed.2025.110453

26. M. Alhazmi, S. Saber, Application of a fractal fractional derivative with a power-law kernel to the glucose-insulin interaction system based on Newton's interpolation polynomials, *Fractals*, 2025. https://doi.org/10.1142/S0218348X25402017

27. S. Saber, B. Dridi, A. Alahmari, M. Messaoudi, Application of Jumarie-Stancu collocation series method and multi-step generalized differential transform method to fractional glucose-insulin, *Int. J. Optimiz. Contro.*, **25** (2025), 464–482. https://doi.org/10.36922/IJOCTA025120054

28. S. Saber, B. Dridi, A. Alahmari, M. Messaoudi, Hyers-Ulam stability and control of fractional glucose-insulin systems, *Eur. J. Pure Appl. Math.*, **18** (2025), 6152. https://doi.org/10.29020/nybg.ejpam.v18i2.6152

29. S. Saber, A. Alahmari, Impact of fractal-fractional dynamics on pneumonia transmission modeling, *Eur. J. Pure Appl. Math.*, **18** (2025), 5901. https://doi.org/10.29020/nybg.ejpam.v18i2.5901

30. M. Althubyani, S. Saber, Hyers-Ulam stability of fractal-fractional computer virus models with the Atangana-Baleanu operator, *Fractal Fract.*, **9** (2025), 158. https://doi.org/10.3390/fractalfract9030158

31. M. Althubyani, H. D. S. Adam, A. Alalyani, N. E. Taha, K. O. Taha, R. A. Alharbi, et al., Understanding zoonotic disease spread with a fractional order epidemic model, *Sci. Rep.*, **15** (2025), 13921. https://doi.org/10.1038/s41598-025-95943-6

32. H. D. S. Adam, M. Althubyani, S. M. Mirgani, S. Saber, An application of Newton's interpolation polynomials to the zoonotic disease transmission between humans and baboons system based on a time-fractal fractional derivative with a power-law kernel, *AIP Adv.*, **15** (2025), 045217. https://doi.org/10.1063/5.0253869

33. S. Saber, E. Solouma, The generalized Euler method for analyzing zoonotic disease dynamics in baboon-human populations, *Symmetry*, **17** (2025), 541. https://doi.org/10.3390/sym17040541

34. S. Saber, E. Solouma, M. Althubyani, M. Messaoudi, Statistical insights into zoonotic disease dynamics: Simulation and control strategy evaluation, *Symmetry*, **17** (2025), 733. https://doi.org/10.3390/sym17050733

35. S. Saber, A. Alahmari, Mathematical insights into zoonotic disease spread: Application of the Milstein method, *Eur. J. Pure Appl. Math.*, **18** (2025), 58–81. https://doi.org/10.29020/nybg.ejpam.v18i2.5881

36. H. Khan, J. Alzabut, A. Shah, S. Etemad, S. Rezapour, C. Park, A study on the fractal-fractional tobacco smoking model, *AIMS Math.*, **7** (2022), 13887–13909. https://doi.org/10.3934/math.2022767

37. S. Saber, A. M. Alghamdi, G. A. Ahmed, K. M. Alshehri, Mathematical modelling and optimal control of pneumonia disease in sheep and goats in Al-Baha region with cost-effective strategies, *AIMS Math.*, **7** (2022), 12011–12049. https://doi.org/10.3934/math.2022669

38. M. Althubyani, N. E. Taha, K. O. Taha, R. A. Alharb, S. Saber, Epidemiological modeling of pneumococcal pneumonia: Insights from ABC fractal-fractional derivatives, *CMES-Comp. Model. Eng.*, **143** (2025), 3491–3521. https://doi.org/10.32604/cmes.2025.061640

39. F. Evirgen, E. Uçar, S. Uçar, N. Özdemir, Modelling influenza a disease dynamics under Caputo-Fabrizio fractional derivative with distinct contact rates, *Math. Model. Numer. Simul. Appl.*, **3** (2023), 58–73. https://doi.org/10.53391/mmnsa.1274004

40. N. Özdemir, E. Uçar, D. Avcı, Dynamic analysis of a fractional SVIR system modeling an infectious disease, *Facta Univ. Ser. Math.*, **37** (2022), 605–619. https://doi.org/10.22190/FUMI211020042O

41. X. P. Li, S. Ullah, H. Zahir, A. Alshehri, M. B. Riaz, B. A. Alwan, Modeling the dynamics of coronavirus with super-spreader class: A fractal-fractional approach, *Results Phys.*, **34** (2022), 105179. https://doi.org/10.1016/j.rinp.2022.105179

42. A. M. Alzubaidi, H. A. Othman, S. Ullah, N. Ahmad, M. M. Alam, Analysis of Monkeypox viral infection with human to animal transmission via a fractional and fractal-fractional operators with power law kernel, *Math. Biosci. Eng.*, **20** (2023), 6666–6690. https://doi.org/10.3934/mbe.2023287

43. A. Atangana, S. I. Araz, Mathematical model of COVID-19 spread in Turkey and South Africa: Theory, methods, and applications, *Adv. Differ. Equ.*, **2020** (2020), 659. https://doi.org/10.1186/s13662-020-03095-w

44. M. Farman, C. Alfiniyah, A. Shehzad, Modelling and analysis of tuberculosis (TB) model with hybrid fractional operator, *Alex. Eng. J.*, **72** (2023), 463–478. https://doi.org/10.1016/j.aej.2023.04.017

45. Z. M. Odibat, C. Bertelle, M. A. Aziz-Alaoui, G. H. E. Duchamp, A multi-step differential transform method and application to non-chaotic or chaotic systems, *Comput. Math. Appl.*, **59** (2010), 1462–1472. https://doi.org/10.1016/j.camwa.2009.11.005

46. H. A. Alkresheh, A. I. Ismail, Multi-step fractional differential transform method for the solution of fractional order stiff systems, *Ain Shams Eng. J.*, **12** (2021), 4223–4231. https://doi.org/10.1016/j.asej.2017.03.017

47. K. Diethelm, N. J. Ford, A. D. Freed, A predictor-corrector approach for the numerical solution of fractional differential equations, *Nonlinear Dyn.*, **29** (2002), 3–22. https://doi.org/10.1023/A:1016592219341

48. L. Sadek, D. Baleanu, M. S. Abdo, W. Shatanawi, Introducing novel Θ-fractional operators: Advances in fractional calculus, *J. King Saud Univ. Sci.*, **36** (2024), 103352. https://doi.org/10.1016/j.jksus.2024.103352

49. L. Sadek, A cotangent fractional derivative with the application, *Fractal Fract.*, **7** (2023), 444. https://doi.org/10.3390/fractalfract7060444

50. L. Sadek, T. A. Lazăr, On Hilfer cotangent fractional derivative and a particular class of fractional problems, *AIMS Math.*, **8** (2023), 28334–28352. https://doi.org/10.3934/math.20231450

51. L. Sadek, O. Sadek, H. T. Alaoui, M. S. Abdo, K. Shah, T. Abdeljawad, Fractional order modeling of predicting COVID-19 with isolation and vaccination strategies in Morocco, *CMES-Comp. Model. Eng.*, **136** (2023), 1931–1950. https://doi.org/10.32604/cmes.2023.025033

52. O. Sadek, L. Sadek, S. Touhtouh, A. Hajjaji, The mathematical fractional modeling of TiO_2 nanopowder synthesis by sol-gel method at low temperature, *Math. Model. Comput.*, **9** (2022), 616–626. https://doi.org/10.23939/mmc2022.03.616

53. A. A. Kilbas, H. M. Srivastava, J. J. Trujillo, *Theory and applications of fractional differential equations*, Elsevier, 2006.

54. Z. Odibat, S. Momani, V. S. Erturk, Generalized differential transform method: Application to differential equations of fractional order, *Appl. Math. Comput.*, **197** (2008), 467–477. https://doi.org/10.1016/j.amc.2007.07.068

55. V. S. Ertürk, Z. M. Odibat, S. Momani, The multi-step differential transform method and its application to determine the solutions of non-linear oscillators, *Adv. Appl. Math. Mech.*, **4** (2012), 422–438. https://doi.org/10.1017/S2070073300001727

56. V. S. Erturk, S. Momani, Z. Odibat, Application of generalized differential transform method to multi-order fractional differential equations, *Commun. Nonlinear Sci.*, **13** (2008), 1642–1654. https://doi.org/10.1016/j.cnsns.2007.02.006

57. Z. Odibat, V. S. Erturk, P. Kumar, A. B. Makhlouf, V. Govindaraj, An implementation of the generalized differential transform scheme for simulating impulsive fractional differential equations, *Math. Probl. Eng.*, **2022** (2022), 8280203. https://doi.org/10.1155/2022/8280203

AIMS Press